

## SHORT COMMUNICATION

**Electrochemical impedance of AgO/Zn and HgO/Zn cells**

M. J. ROOT

*Rayovac Corporation, PO Box 44960, Madison, WI 53744-4960 USA*

Received 24 January 1995; revised 15 August 1995

**1. Introduction**

Porous electrodes are important features in electrochemical power sources. They provide high electrode surface areas in contact with the electrolyte which helps to maximize the currents that may be drawn under load and promote efficient utilization of the electrode.

Electrochemical impedance (EI) is becoming a widely used method for evaluation of porous materials and electrochemical power sources. It is an essentially nondestructive technique which in many cases can be used to probe an electrochemical system as a function of composition or discharge state. In the best cases, the characteristics of individual cell components (anode, separator and cathode) may be distinguished, expanding the diagnostic utility of EI.

In this work, the impedance spectra of some AgO/Zn and HgO/Zn 'button' cells were measured. This is an important class of cell used to power small devices such as watches and hearing aids [1]. The cathodes of these cells, like many other cell types, are comprised of a metal oxide powder compressed into a pellet. Electrolyte fills the pores between the cathode particles. This results in a consolidated, porous electrode that optimizes material density while maintaining extensive surface exposure to the electrolyte.

**2. Experimental details**

Commercially available AgO/Zn (312, 13 and 675 sizes) and HgO/Zn cells (13 size) were used for all experiments. Cell dimensions for the different sizes are given in Table 1. These cells were chosen because two of the cells (and their cathodes) had similar diameters but different heights, and two had similar heights but different diameters. The AgO cathodes are a mixture of AgO with minor amounts of Ag<sub>2</sub>O, Ag<sub>5</sub>Pb<sub>2</sub>O<sub>6</sub> and Ag [1]. These cells contain the cathode powder pressed into a pellet, separators and an anode containing zinc particles. Three electrode measurements with 13 size AgO/Zn cells were performed using a Hg/HgO (38% KOH/3% ZnO) reference electrode. The side of a cell was abraded with SiC paper until the cathode was exposed and a small hole was drilled by hand into the cathode to accept a Luggin probe. The probe contained an electrolyte gel (prepared with polyacrylic acid and an aqueous 38% KOH/3% ZnO solution). All experiments were run at ambient temperature.

Impedance spectra were obtained with an EG&G PAR 273A potentiostat served by a Solartron Instruments 1255 frequency response analyser. Data were collected using EG&G model 288 software. Measurements were made at the open circuit potential with a superimposed 5 mV sinusoidal voltage in the frequency range  $2.2 \times 10^{-4}$  to  $1 \times 10^5$  Hz.

Experimental real and imaginary impedance data were fitted using an equation of the form:

$$Z_{\text{calc}} = a_0 + a_1(j\omega)^{-a_2} \coth[a_3(j\omega)^{a_2}] \quad (1)$$

where  $Z_{\text{calc}}$  is the calculated complex impedance,  $a_n$  are the fit parameters,  $j = \sqrt{-1}$  and  $\omega$  is the angular frequency. Calculations were performed with a fitting program written using Igor (WaveMetrics). The fitting procedure sought to minimize the sum of the squares of the differences between observed real ( $Z'_{\text{obsd}}$ ) or imaginary ( $Z''_{\text{obsd}}$ ) impedances and the corresponding calculated values  $Z'_{\text{calc}}$  and  $Z''_{\text{calc}}$  from Equation 1; each term was weighted using  $1/Z'_{\text{obsd}}$  or  $1/Z''_{\text{obsd}}$  [2]:

$$\left( \frac{Z'_{\text{obsd}} - Z'_{\text{calc}}}{Z'_{\text{obsd}}} \right)^2 + \left( \frac{Z''_{\text{obsd}} - Z''_{\text{calc}}}{Z''_{\text{obsd}}} \right)^2 \quad (2)$$

Only the lowest frequencies,  $8.6 \times 10^{-3}$  Hz to 4.0 Hz  $\leq \omega/2\pi \leq 2.2 \times 10^{-4}$  Hz, were used, depending on cell type and size. Data at higher frequencies included contributions from the anode and separator. Errors are shown as standard deviations.

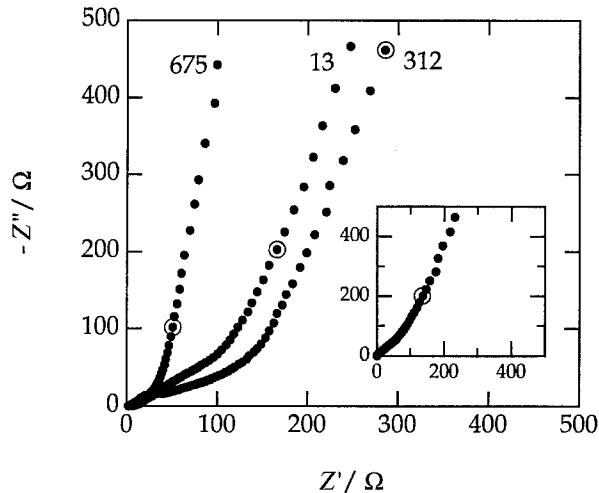
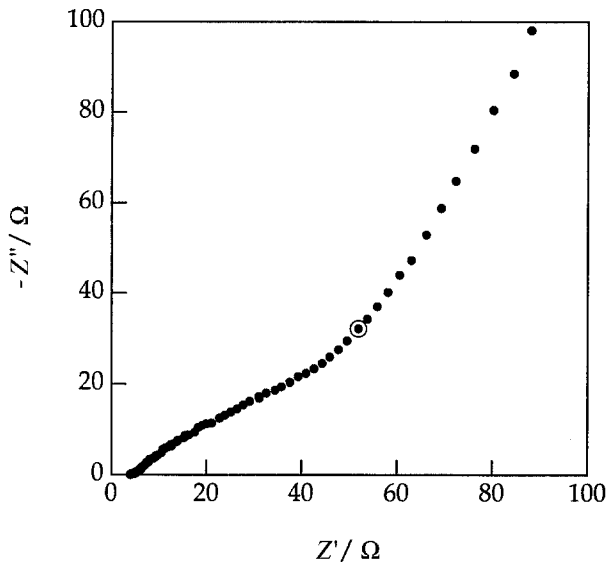
**3. Results and discussion**

Typical complex plane impedance plots for AgO/Zn 312, 13 and 675 cells and a HgO/Zn 13 cell are shown in Figs 1 and 2, respectively. The spectra are qualitatively similar: the high frequency portion of the spectra shows broad, poorly defined peaks while two linear regions are evident at low frequencies.

One of the advantages of EI is the capability of measuring simultaneous processes occurring at disparate reaction rates. In the best cases, this can mean that impedance behaviour of the anode and cathode of electrochemical power sources may be distinguished. The inset in Fig. 1 displays the cathode spectrum (measured using a Hg/HgO reference electrode) of a AgO/Zn 13 cell. The data match the low frequency features of the cell spectra. Likewise, the data in Fig. 2 for frequencies  $> 1 \times 10^{-2}$  Hz are rather similar to complex plane impedance plots shown in a previous EI study using cylindrical HgO/Zn cells measured at frequencies  $> 1 \times 10^{-2}$  Hz [3]. In that work, the observed impedance data were

Table 1. Cell dimensions for 312, 13 and 675 AgO/Zn cells

Cell designation	Diameter/cm	Height/cm
312	0.79	0.36
13	0.78	0.54
675	1.16	0.54

Fig. 1. Complex plane impedance plots for AgO/Zn 312, 13 and 675 cells. Inset: complex plane impedance plot for AgO cathode in AgO/Zn 13 cell. Circled data points:  $f = 1.4 \times 10^{-3}$  Hz.Fig. 2. Complex plane impedance plot for a HgO/Zn 13 cell. Circled datum point:  $f = 1.4 \times 10^{-3}$  Hz.

attributed to the anode. Thus, as may be noted by comparing the curves in Figs 1 and 2 and the literature report [3], the low frequency linear regions of the cell spectra can be assigned to the cathode impedance. The high frequency features are taken to be derived from the anode and separator.

Following Paasch *et al.* [4], the impedance of an electroactive porous electrode may be described by Equation 3,

$$ZA = \left( \frac{\rho_1^2 + \rho_2^2}{\rho_1 + \rho_2} \right) \left( \frac{\coth(l\beta_1)}{\beta_1} \right) + \left( \frac{2\rho_1\rho_2}{\rho_1 + \rho_2} \right) \times \left( \frac{1}{\beta_1 \sinh(l\beta_1)} \right) + \left( \frac{l\rho_1\rho_2}{\rho_1 + \rho_2} \right) \quad (3)$$

where  $A$  is the electrode area,  $\rho_1$  and  $\rho_2$  are the electronic and ionic resistivities of the solid and pore electrolyte phases, respectively, and  $\beta_1 = [(k + j\omega)/K_1]^{1/2}$ . The constants  $K_1$  and  $k$  incorporate charge transfer and double layer capacitance terms:  $k = I_0 n F / C_{dl} R T$  and  $K_1 = 1 / C_{dl} S (\rho_1 + \rho_2)$ , where  $I_0$  is the exchange current density,  $C_{dl}$  is the double layer capacitance per unit interface area,  $S$  is the area of the pores per unit volume and  $n$ ,  $F$ ,  $R$  and  $T$  have their usual meanings. The length of the porous electrode,  $l$ , is referred to as the cathode height here.

The presence of electronically conductive material in the cathode permits the assumption of negligible solid phase resistivity ( $\rho_1 = 0$ ). Further, if the charge transfer kinetics are slow, then  $k$  is insignificant and Equation 3 becomes.

$$ZA = \frac{\rho_2 \coth(l\beta_2)}{\beta_2} \quad (4)$$

where now  $\beta_2 = (j\omega/K_2)^{1/2}$  and  $K_2 = 1/C_{dl} S \rho_2$ .

Using Equation 4, two linear regions in the complex plane impedance plot are observed: a line with unit slope at higher frequencies and a line with infinite slope at lower frequencies. The spectra in Fig. 1 show negative deviations from this ideal behaviour indicating a fractional power dependence, so  $l\beta_2$  was replaced with  $[B(j\omega)^\xi]^{1/2}$ .  $B$  may be considered to be a kind of time constant and  $\xi$  has a value between 0 and 1. This type of treatment has been used previously by including an empirical constant phase element parameter [2] or employing a fractal model [5] to account for nonuniform system properties.

Figure 3 overlays the measured and fit complex plane impedance plots for a AgO/Zn 13 cell and indicates a satisfactory fit at low frequencies using Equation 1. Calculated values for each of the fit parameters are dependent on cell type and size. The  $a_0$  term from Equation 1 contains the cell ohmic resistance (usually dominated by the bulk electrolyte resistance) along with anode and separator impedances. From Equations 1 and 4,  $a_1 = \rho_2 l / B^{1/2}$ ,  $a_2 = \xi / 2$  and  $a_3 = B^{1/2}$ .

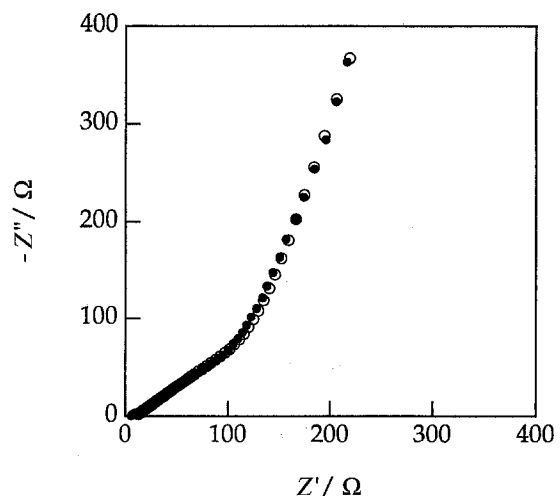


Fig. 3. Complex plane impedance plot for a AgO/Zn 13 cell and the resulting fit. Key: (●) observed data; (○) calculated data.

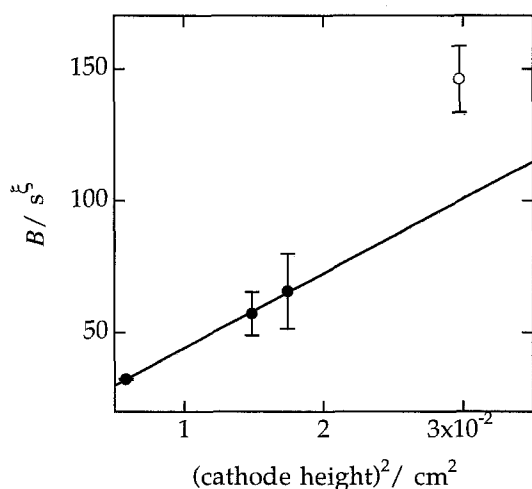


Fig. 4. Plot of  $B$  against square of cathode height for AgO/Zn 312, 13 and 675 cells and HgO/Zn 13 cells. Key: (●) AgO/Zn, (○) HgO/Zn.

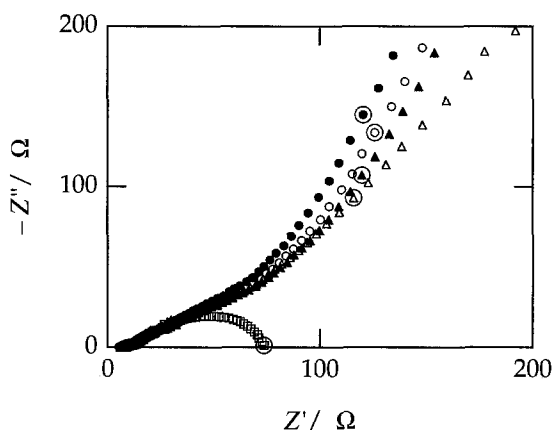


Fig. 5. Complex plane impedance plots for a AgO/Zn 13 cell as a function of applied voltage: (●) open circuit voltage (1.703 V), (○) 1.650 V, (▲) 1.600 V, (△) 1.575 V, (□) 1.555 V. Circled data points:  $f = 2.2 \times 10^{-3}$  Hz.

Measured impedance values scale inversely with the geometric area of the electrode, as expected (Equations 3 and 4). In Equation 4,  $l\beta_2 (= l(j\omega/K_2)^{1/2})$  is replaced with  $[B(j\omega)^\xi]^{1/2}$  to account for nonideal factors. Comparing these ideal and nonideal terms reveals that  $B$  should be linearly dependent on the square of the cathode height. Figure 4 suggests this is indeed the case for the three AgO/Zn cell sizes tested.

Complex plane impedance plots for a 13 cell at various applied voltages is shown in Fig. 5. There was no indication of charge transfer occurring at or near open circuit voltages at frequencies to  $2 \times 10^{-4}$  Hz. As the applied voltage is decreased and the cell is discharged (Fig. 5) the low frequency complex impedance values gradually curve towards the real impedance axis implying that significant charge transfer occurs at  $< 1.6$  V. This result is predicted by Equation 4 when  $\beta_2$  is replaced by  $\beta_1$ , which would then account for charge transfer.

As seen in Fig. 4, HgO/Zn 13 cells have larger  $B$  values when compared to similarly sized AgO/Zn cells. It would be difficult to speculate on the reasons for these differences based on the limited data from this study, but may be related to larger  $C_{dl}$ ,  $S$  or  $\rho_2$  values.

#### 4. Conclusions

EI offers a way to assess modifications in cathode material, processing and cell design, or identify problems that affect cell performance. It was found that a porous electrode model including double layer capacitance and pore electrolyte resistance, modified by the inclusion of terms that describe inhomogeneities, may be used to calculate impedance parameters that are a function of cell type and dimensions for AgO/Zn cells. Comparison of these impedance parameters for test cells with those for control cells may point to specific areas for improvements, including the electrolyte and cathode processing.

#### References

- [1] E. A. Megahed, in 'Modern Battery Technology', Ellis Horwood, Chichester, UK (1991).
- [2] J. R. Macdonald (ed.), 'Impedance Spectroscopy', John Wiley & Sons, New York (1987).
- [3] S. A. G. R. Karunathilaka, N. A. Hampson, T. P. Haas, R. Leek and T. J. Sinclair, *J. Appl. Electrochem.* **11** (1981) 573.
- [4] G. Paasch, K. Micka and P. Gersdorf, *Electrochim. Acta* **38** (1993) 2653.
- [5] R. de Levie, *J. Electroanal. Chem.* **281** (1990) 1.